Stanford Exploration Project, Report 112, November 11, 2002, pages 109–117

Short Note

Equivalence of source-receiver migration and shot-profile migration

Biondo Biondi[1]

INTRODUCTION

At first glance, shot profile migration and source-receiver (survey-sinking) migration seem to be substantially different algorithms. The basic principles used by the two schemes are different. Shot profile migration is performed by *independently* propagating the source wavefield and the receiver wavefield. The image is obtained by cross-correlating (possibly normalized by the amplitude of the source wavefield) the two wavefields. Source-receiver migration is based on the concept of survey sinking, by which we recursively synthesize equivalent data sets at increasing depth. At each depth step imaging is performed by extracting the wavefield at zero time.

The issue of the relation between shot-profile migration and source-receiver migration has become more relevant since the recent introduction of methods for computing angle-domain common image gathers for source-receiver migration (Prucha et al., 1999; Sava et al., 2001). Rickett and Sava (2002) extended one of these methods [(Sava et al., 2001)] to downward-continuation shot-profile migration, and Biondi and Shan (2002) extended it to reverse-time shot-profile migration. Their extensions depend on the "equivalence" of the offset-domain common image gathers computed by shot-profile migration and source-receiver migration.

In this short note I demonstrate that the two migration methods produce exactly the same image cube; that is, the images are the same not only at zero subsurface offset, but also at non-zero subsurface offset. Wapenaar and Berkhout (1987) had already demonstrated the same result. Their focus, however, was on the stacked image, not on the whole image cube.

For the identity of the two methods to hold, the shot profile migration needs to satisfy three specific requirements: 1) the source function is an impulse at zero time and it has no spatial width, 2) the imaging condition is the cross-correlation of the source wavefield by the receiver wavefield, 3) the source and receiver wavefields are propagated by downward continuation. Another obvious assumption is that the same numerical algorithm is employed to downward continue the wavefields for both migration methods.

[1]**email:** biondo@sep.stanford.edu

The demonstration of the equivalence of the two migration methods becomes fairly simple when we consider the migration of a single shot record by source-receiver downward continuation. In this case, the downward continuation of the sources is equivalent to the multiplication of the downward-continued receiver wavefield with many copies of the complex conjugate (time reversed) source wavefield appropriately shifted along the receiver axis.

THEORY

I first review the basic principles of shot-profile migration and source-receiver migration. Then I will show their equivalence.

Shot-profile migration

In shot-profile migration each record is migrated independently. The receiver wavefield P^g is downward continued starting from the recorded data. The source wavefield $P^s$is downward continued starting from an assumed source wavelet. In this case, we assume that the source is a delta function in the space domain and a constant as a function of frequency (impulse at time zero).

Each wavefield is propagated independently by convolution with the Single Square Root operator (SSR). At each depth level that is;

$$ {}^{\delta}P_z^s(\omega,x,y;\mathbf{s}) = \delta(x-x_s,y-y_s) \overset{x,y}{*} e^{-ik_z z}. \tag{1}$$

and

$$ P_z^g(\omega,x,y;\mathbf{s}) = P_{z=0}^g(\omega,x,y;\mathbf{s}) \overset{x,y}{*} e^{ik_z z}, \tag{2}$$

where x and y are defined in the image (model) space, and $\mathbf{s}=(x_s,y_s)$ is the location of the shot. The prefix δ in ${}^{\delta}P_z^s$ indicates that the source function is an impulse. Notice the negative sign in front of the exponential in equation (1). The negative sign is there because the source wavefield propagates downward, as opposed to propagate upward as the receiver wavefield does.

The image cube is formed by cross-correlating along the time axis the two wavefields shifted with respect to each other along the horizontal axes. In the frequency domain the cross-correlation is performed by multiplication with the complex conjugate, and it is evaluated at zero lag by summation over frequencies. The horizontal shift is the subsurface offset (x_h,y_h). The image cube is thus computed as:

$$ I_{\text{shot}}(z,x,y,x_h,y_h) = \sum_{x_s}\sum_{y_s}\sum_{\omega} P_z^g(\omega,x+x_h,y+y_h;\overline{\mathbf{s}})\,\overline{{}^{\delta}P_z^s(\omega,x-x_h,y-y_h;\overline{\mathbf{s}})} \tag{3}$$

Source-receiver migration

Source-receiver migration is based on the concept of survey sinking. After each depth propagation step, the propagated wavefield is equivalent to the data that would have been recorded

if all sources and receivers were placed at the new depth level. This task is accomplished by downward continuing all the source and receiver gathers at each depth step. Therefore, the basic downward continuation is performed by convolving with the Double Square Root (DSR) equation, as

$$P_z(\omega,\mathbf{g},\mathbf{s}) = P_{z=0}(\omega,\mathbf{g},\mathbf{s}) \overset{\mathbf{g}}{*} e^{ik_z z} \overset{\mathbf{s}}{*} e^{ik_z z}, \tag{4}$$

where the first convolution downward-continues the receiver wavefield, whereas the second convolution downward-continues the receiver wavefield. Notice the positive sign on both exponentials in equation (4).

At each depth level, the image is extracted from the downward-continued wavefield by evaluating the wavefield at zero time. The image-space coordinates and the source-receiver coordinates are linked by the well-known transformations

$$\begin{aligned} x_s &= x - x_h \qquad & x_g &= x + x_h \\ y_s &= y - y_h \qquad & y_g &= y + y_h. \end{aligned} \tag{5}$$

The image cube is then computed as

$$I_{\mathrm{s-g}}(z,x,y,x_h,y_h) = \sum_{\omega} P_z(\omega, x+x_h, y+y_h, x-x_h, y-y_h) \tag{6}$$

Equivalence of source-receiver migration and shot-profile migration

For the sake of simplicity, I demonstrate the equivalence by showing that the images obtained by migrating a single shot record are the same. The linearity of both migrations with respect to the input wavefield makes the extension to the full data set obvious.

A crucial observation for proving the equivalence of the two migration methods is that the downward continuation of the sources commutes with the downward continuation of the receivers. This property is obvious for vertically layered media where downward continuation can be performed in the wavenumber domain. However, it is also valid in presence of lateral velocity variations, because the wavefield is downward-continued along each direction by a convolution that is independent from the other direction. For example, the sources are downward continued by convolving each receiver gather with a convolutional operator that is non-stationary along the source axis, but is independent of the location of the receiver gather.

The wavefield at the surface for one single shot gather is given by the products of two functions: the first is independent of the source-coordinate $\mathbf{s}$ (the recorded data $P^g_{z=0}(\omega,\mathbf{g};\bar{\mathbf{s}})$), the second is independent of the receiver-coordinate $\mathbf{g}$ (a delta function at $\bar{\mathbf{s}}$).

The wavefield at depth obtained by survey sinking can thus be expressed as

$$\begin{aligned} & P_z(z,\mathbf{g},\mathbf{s}) \\ &= \left[P^g_{z=0}(\omega,\mathbf{g};\bar{\mathbf{s}})\,\delta(\mathbf{s}-\bar{\mathbf{s}})\right] \overset{\mathbf{g}}{*} e^{ik_z z} \overset{\mathbf{s}}{*} e^{ik_z z} \end{aligned}$$

$$= \left[P^g_{z=0}(\omega,\mathbf{g};\overline{\mathbf{s}}) \overset{\mathbf{g}}{*} e^{ik_z z}\right]\left[\delta(\mathbf{s}-\overline{\mathbf{s}}) \overset{\mathbf{s}}{*} e^{ik_z z}\right]$$
$$= \left[P^g_z(\omega,\mathbf{g};\overline{\mathbf{s}})\right]\left[\overline{{}^{\delta}P^s_z(\omega,x_s,y_s;\overline{\mathbf{s}})}\right]. \qquad (7)$$

Imaging is performed by evaluating the downward-continued wavefield at the appropriate locations, as described by equation (6). If we apply this imaging condition to the wavefield in (7), we obtain

$$I_{\mathrm{s-g}}(z,x,y,x_h,y_h) = \sum_{\omega}\left[P^g_z(\omega,x+x_h,y+y_h;\overline{\mathbf{s}})\right]\left[\overline{{}^{\delta}P^s_z(\omega,x-x_h,y-y_h;\overline{\mathbf{s}})}\right], \qquad (8)$$

that is exactly the same image cube as the image cube obtained by shot-profile migration [equation (3)].

TESTS ON SYNTHETIC DATA SET

To test the theoretical result reached in the previous section I migrated one shot record from a synthetic data modeled over a medium with strong lateral velocity variations that cause the image produced by migrating a single shot to have coherent artifacts. The test is useful both to demonstrate that in the source-receiver migration the downward continuation along the shot axis and along the receiver axis do indeed commute in presence of strong lateral variations. It is also interesting to confirm that the migration artifacts produced by source-receiver migration and shot profile migration are the same. The data set was kindly provided by Bill Symes of Rice University, and it has been used to study the artifacts produced by different kind of migrations (Stolk and Symes, 2002). The reflector geometry is a simple flat reflector, but a strong velocity anomaly above it creates severe multipathing that challenges different migration schemes.

The theoretical result is based on the assumption that the numerical algorithm used to propagate the wavefield is exactly the same. Unfortunately, SEP still lacks a downward-continuation shot-profile migration capable of handling severe velocity variations, though Brad Artman is close to succeeding in getting one up and running (2002). Therefore, for the moment I had to run an "imperfect" test and I compare the results of migrating synthetic data by source-receiver downward continuation and reverse-time shot-profile migration (Biondi and Shan, 2002).

Figure 1 shows the shot with source location at .5 kilometers used for the test. Figure 2 shows the zero offset (stack) image produced by both migrations methods. The panel on the left shows the image produced by shot-profile migration, and the panel on the right shows the image produced by source-receiver migration. The two images are similar, except for a small difference in frequency content caused by the fact that I did not enter a perfect impulsive source in the shot-profile migration to avoid dispersion. Not only the flat reflector is imaged similarly in the two images, but also the strong "ghost" reflectors caused by the triplication of the wavepath (Valenciano and Biondi, 2002), visible between the surface locations of 0 and 1 km, are almost identical.

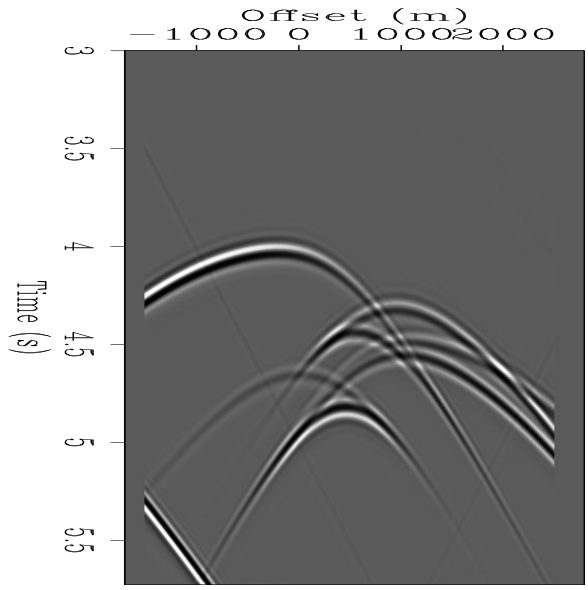

Figure 1: Shot profile used for the tests. biondo2-Shot-trip [CR]

Figure 3 shows the subsurface offset-domain common image gathers at the surface location of 300 meters: panel a) shot-profile migration, panel b) source-receiver migration). Again the images are similar for both the "true" reflector and the "ghost" reflectors. Figure 4 shows the angle-domain common image gathers obtained from the offset-domain gathers shown in Figure 3 after a slant stack transformation (Sava et al., 2001). Notice that the "true" reflector gets imaged at both positive and negative aperture angle because of the wavepath triplications. The "ghost" reflectors get imaged in the aperture-angle gap between the two branches of the true reflector.

Figure 5 demonstrates that the artifacts disappear if the whole data set (400 shots) is imaged. It shows the zero offset image [panel a)] and the angle-domain common image gather [panel b)] obtained by source-receiver migration when all the shot records are included in the data. I did not migrate all the shots by reverse time migration, because it would have taken considerable computer resources.

CONCLUSIONS

I have proven theoretically that source-receiver migration is exactly equivalent to downward-continuation shot-profile migration.

The results of the migration tests that I show strongly support this theoretical result, though they are not the ultimate proof, since I was limited to run a reverse-time shot-profile migration instead of a downward-continuation shot-profile migration.

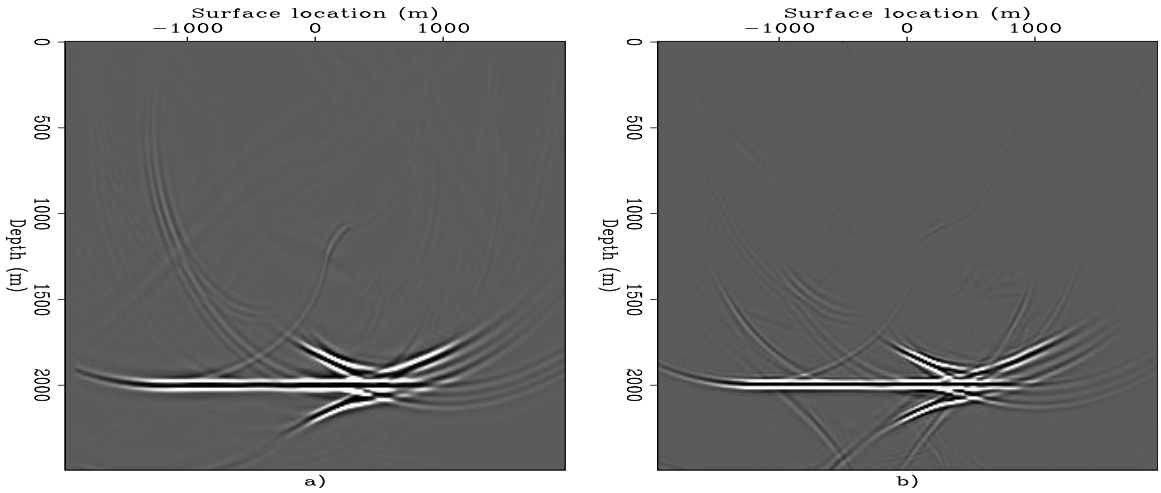

Figure 2: Zero-offset sections of the migrated cubes obtained using: a) shot-profile reverse-time migration, b) source-receiver downward-continuation migration. biondo2-Mig-trip-both [CR]

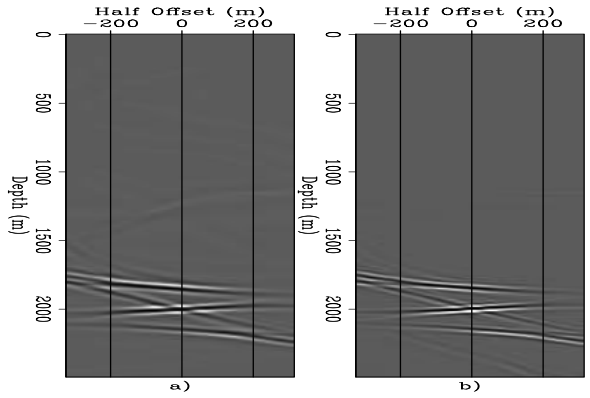

Figure 3: Offset-domain common image gathers obtained by slicing the migrated cubes at the surface location of 100 meters: a) shot-profile reverse-time image, b) source-receiver downward-continuation image. biondo2-Cig-trip-100-both [CR]

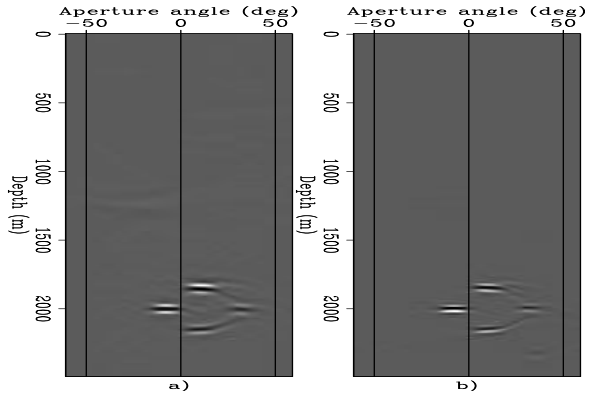

Figure 4: Angle-domain common image gathers obtained by slicing the migrated cubes at the surface location of 100 meters: a) shot-profile reverse-time image, b) source-receiver downward-continuation image. biondo2-Ang-Cig-trip-100-both [CR]

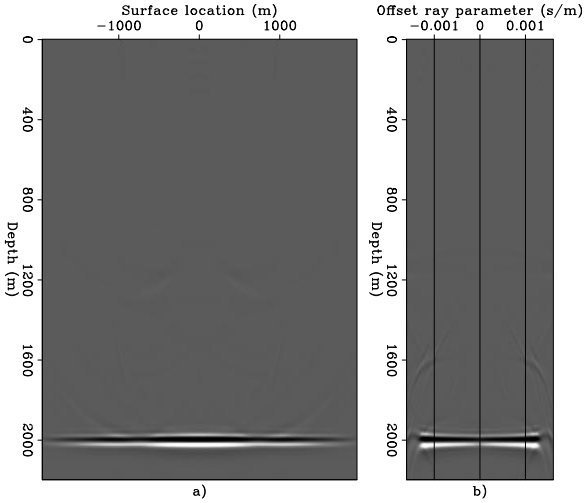

Figure 5: Stacked image (panel a)) and angle-domain common image gather at surface location of 100 meters (panel b)) obtained by source-receiver downward-continuation migration of the whole data set (400 shots). biondo2-Mig-Ang-Cig-trip-300-sr-full [CR]

ACKNOWLEDGMENTS

I would like to thank Bill Symes of Rice University for kindly providing the synthetic data set that was used for the tests shown in the paper.

REFERENCES

Artman, B., 2002, Migrating passive seismic data: SEP–**112**, 131–136.

Biondi, B., and Shan, G., 2002, Prestack imaging of overturned reflections by reverse time migration: 72nd Ann. Internat. Meeting, Soc. of Expl. Geophys., Expanded Abstracts, to be published.

Prucha, M., Biondi, B., and Symes, W., 1999, Angle-domain common-image gathers by wave-equation migration: 69th Ann. Internat. Meeting, Soc. Expl. Geophys., Expanded Abstracts, 824–827.

Rickett, J., and Sava, P., 2002, Offset and angle-domain common image-point gathers for shot-profile migration: Geophysics, **67**, 883–889.

Sava, P., Biondi, B., and Fomel, S., 2001, Amplitude-preserved common image gathers by wave-equation migration: 71st Ann. Internat. Meeting, Soc. Expl. Geophys., Expanded Abstracts, 296–299.

Stolk, C., and Symes, W., 2002, Artifacts in Kirchhoff common image gathers: 72nd Ann. Internat. Meeting, Soc. of Expl. Geophys., Expanded Abstracts, to be published.

Valenciano, A. A., and Biondi, B., 2002, Deconvolution imaging condition for reverse-time migration: SEP–**112**, 83–96.

Wapenaar, C. P. A., and Berkhout, A. J., 1987, Full prestack versus shot record migration: 69th Ann. Internat. Meeting, Soc. of Expl. Geophys., Expanded Abstracts, Session:S15.7.